Applied Catalysis B: Environmental 301 (2022) 120767

Contents lists available at ScienceDirect

Applied Catalysis B: Environmental

journal homepage: www.elsevier.com/locate/apcatb

Self-hydrogen transfer hydrogenolysis of native lignin over Pd-PdO/TiO_2

Zhaolin Dou, Zhe Zhang, Min Wang *

Zhang Dayu School of Chemistry, Dalian University of Technology, Dalian 116024, Liaoning, China

A B S T R A C T

Lignin is a renewable aromatics resource that can be converted into high-value chemicals through the β-O-4 linkage cleavage. Self-hydrogen transfer hydrogenolysis (STH) is a promising way to produce monomers from lignin through the β-O-4 linkage cleavage with no additional hydrogen sources, but usually with low yield toward native lignin. Here, a Pd-PdO/TiO_2 catalyst was prepared for the STH of native lignin. Compared with Pd/TiO_2 and PdO/TiO_2, Pd-PdO/TiO_2 showed the highest activity in the STH of C_β−O bond in β-O-4 models. In the STH process, the C_αH-OH in β-O-4 linkage is dehydrogenated to form β-O-4 ketone intermediates, and hydrogens are adsorbed on Pd sites to form a "hydrogen pool" which participates in the following hydrogenolysis of C_β−O bond. DFT calculation shows that PdO more effectively activates the β-O-4 ketone intermediate and shows lower activation energy toward C_β−O bond cleavage compared with Pd. Pd acts as the dehydrogenation site and PdO activates the C_β−O bond. The co-existence of Pd and PdO facilitates the C_β−O bond cleavage of β-O-4 linkage and about 40 *wt* % yields of lignin monomers can be obtained from poplar lignin at 180 °C.

1. Introduction

Lignin, part of lignocellulosic biomass, which is formed by the photosynthesis of plants, is the most abundant renewable aromatic biopolymer [1,2]. Depolymerization of lignin into high value-added chemicals especially aromatics has drawn many researchers' attention in recent years [3–11]. Lignin has a very complex 3D structure, which is formed by the polymerization of three monomers (coumaryl, coniferyl and sinapyl alcohols) [1,12,13]. β-O-4 linkage is the dominant linkage, which accounted for 43–62% in native lignin [14,15]. The cleavage of β-O-4 linkage is the key for lignin depolymerization.

Hydrogenolysis is the most efficient way for the C-O bond cleavage of β-O-4 linkage, which usually requires hydrogen or a hydrogen donor as the reductant, and uses the heterogenous metal catalyst, including Ni [16–24], Pt [25–27], Ru [28–31], and Pd [32–38]. Recently, a self-hydrogen transfer hydrogenolysis (STH) strategy has emerged as a promising way to depolymerize lignin into monomers with no additional hydrogen sources, which use hydroxyl groups in lignin itself as the hydrogen donor [39]. Bergman and Ellman [39] initially developed a homogeneous, phosphine-ligated Ru catalyst to cleave a β aryl ether model compound. Cai [40] and coworkers reported a MIL-100 (Fe) supported Pd-Ni bimetal nanoparticles for the STH of lignin model compounds and organosolv lignin. The photocatalytic method for the STH of lignin models was realized over $ZnIn_2S_4$ [41] and CdS photocatalyst [42]. More recently, a self-reforming-driven depolymerization and hydrogenolysis strategy to get 4–alkylphenols from native lignin was reported [43], which generates 17.3 *wt* % of 4–alkylphenols from birch lignin at 280 °C in 20 h. However, these methods usually focus on the STH of lignin model compounds or show a low monomer yield of STH toward native lignin.

Herein, we report STH of native lignin to monomers over Pd-PdO/TiO_2 catalyst. Compared with Pd/TiO_2 and PdO/TiO_2, Pd-PdO/TiO_2 showed enhanced activity for the STH of the C_β-O bond in β-O-4 models. With Pd-PdO/TiO_2 as the catalyst, 40 *wt* % yields of lignin monomers were produced from poplar lignin without additional hydrogen sources at 180 °C. Pd acts as the dehydrogenation site and PdO activates the C_β-O bond. The co-existence of Pd and PdO facilitates the C_β-O bond cleavage of β-O-4 linkage.

2. Experimental section

2.1. Catalyst preparation

The PdO/TiO_2 catalyst was prepared by the deposition-precipitation method. Typically, 475 mg of TiO_2 was dissolved in 20 mL of water in a 100 mL beaker and magnetically stirred at room temperature. Then, 25 mg of Pd (4.136 mL $PdCl_3$/HCl solution) was added into the above suspension and stirred for one minute. After the suspension got uniform, 1 M NaOH (aq.) was added into the mixture to adjust its pH to 8. Then the suspension was stirred for 24 h. After being washed with deionized water 6 times, a brown solid was obtained. And the solid was dried at 60 °C for 12 h to get PdO/TiO_2. Pd-PdO/TiO_2 was prepared by the following reduction process. The as-prepared PdO/TiO_2 was reduced by H_2 at room temperature to get Pd-PdO/TiO_2. And for comparison, PdO/

* Corresponding author.
E-mail address: wangmin@dlut.edu.cn (M. Wang).

https://doi.org/10.1016/j.apcatb.2021.120767
Received 30 June 2021; Received in revised form 22 September 2021; Accepted 26 September 2021
Available online 29 September 2021

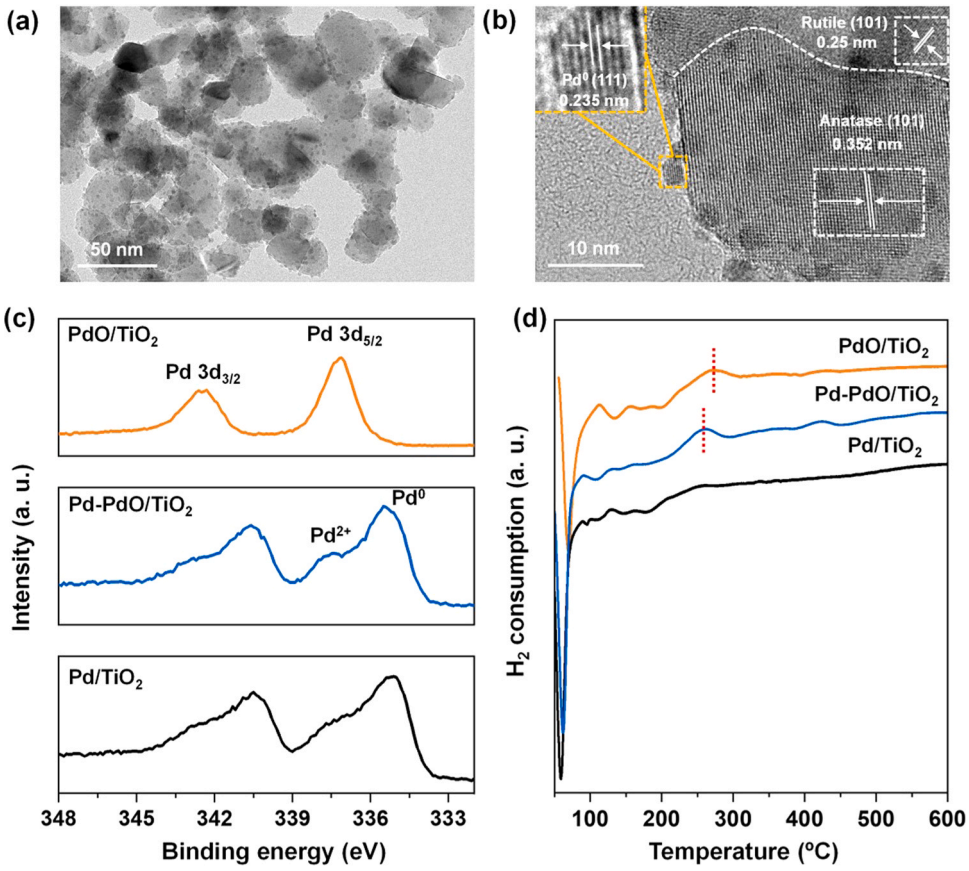

Fig. 1. Structure characterization of catalyst. (a), (b) HR-TEM images of Pd-PdO/TiO_2. (c) XPS spectra of PdO/TiO_2, Pd-PdO/TiO_2 and Pd/TiO_2. (d) H_2-TPR spectra of PdO/TiO_2, Pd-PdO/TiO_2 and Pd/TiO_2.

TiO_2 was reduced by H_2 at 400 °C to get Pd/TiO_2. The theoretical content of Pd in the as-prepared catalyst is 5 *wt* %. And the actual content of Pd in the catalyst is 3.4 *wt* %, which is determined from ICP measurement.

2.2. STH of lignin model compounds and native lignin

Typically, 20 mg of lignin model compound including 2-phenoxy-1-phenylethanol, 2-(2-methoxyphenoxy)-1-phenylethanol, 1-(4-methoxyphenyl)-2-(2-methoxyphenoxy) ethanol, 2-(2,6-dimethoxyphenoxy)-1-phenylethanol, α-[(2,6-dimethoxyphenoxy) methyl]-4-methoxybenzene methanol and 1-(3,4-dimethoxyphenyl)-2-(2-methoxyphenoxy) ethanol, 2 mL of water, 5 mg of catalyst, were added into a 20 mL autoclave reactor with an internal Teflon insert. Then the stainless-steel autoclave was heated to a certain temperature under magnetic string in Ar atmosphere. For the depolymerization of native lignin, 500 mg of wood sawdust, 50 mg of Pd-PdO/TiO_2, 10 mL of water were added into a 50 mL autoclave reactor with an internal Teflon insert and heated to 180 °C for 6 h under magnetic string in Ar atmosphere. After the reaction, the reactants and products were analyzed by gas chromatography-mass spectrometry (GC-MS) using an Agilent 7890 A/5975 C instrument equipped with an HP-5 MS column (30 m in length, 0.25 mm in diameter), and quantified by gas chromatography using an Agilent 8860 instrument equipped with an HP-5 MS column (30 m in length, 0.25 mm in diameter) and FID detector. The conversion and yields were determined using an internal standard method. The detailed calculation was illustrated in Supporting Information.

2.3. General characterizations

X-ray diffraction (XRD) patterns of the as-prepared catalysts were conducted with a Smartlab 9 kW (Rigaku Corporation) diffractometer, using Cu-Kα radiation at 45 kV and 200 mA. The 2-theta range was scanned from 20° to 90°. Transmission electron microscopy (TEM) images were collected using a Titan G2 60–300 (American, FEI) operating at 200 kV. X-ray photoelectron spectra (XPS) measurements were carried on Thermo Fischer ESCALAB Xi+ spectrometer equipped with an Al Kα X-ray source (hυ = 1486.8 eV, 12.5 kV, 16 mA). The analysis base pressure was 8×10^{-10} Pa. The passing energy was 20 eV and the 0.05 eV step was used to acquire the data. The charge correction of binding energy was conducted with the C1s = 284.80 eV. H_2-temperature-programmed reduction (H_2-TPR) experiments were conducted on the VDSorb-91i chemical adsorption apparatus (Quzhou Vodo Instrument Co., Ltd.) with a quartz U-tube reactor. For the detail of the experiment, 0.1 g of the catalysts were heated under ultra-high purity Ar flow (15 sccm) up to 250 °C at 15 °C/min for 1 h to remove the water. After cooling down to room temperature, H_2/Ar (10% H_2) mixture flow (15 sccm) passed through the sample the temperature of the reactor was raised to 800 °C with the rate of 15 °C/min. The H_2-TPR data was recorded during the heating.

2.4. DFT calculations

All of the first-principles electronic structure calculations were carried out using the Vienna ab initio simulation package (VASP) [44], one density functional theory implementation. The exchange correlation potential was described by the Perdew–Burke–Ernzerhof (PBE) formulation of the generalized gradient approximation (GGA) [45]. The ion–electron interactions were represented by the projector augmented wave (PAW) [46] method. A plane wave basis set with an energy cutoff of 400 eV was used. The *k*-point sampling was performed using the Monkhorst–Pack scheme [47]. The electronic self-consistent minimization was converged to 10^{-5} eV, and the geometry optimization was

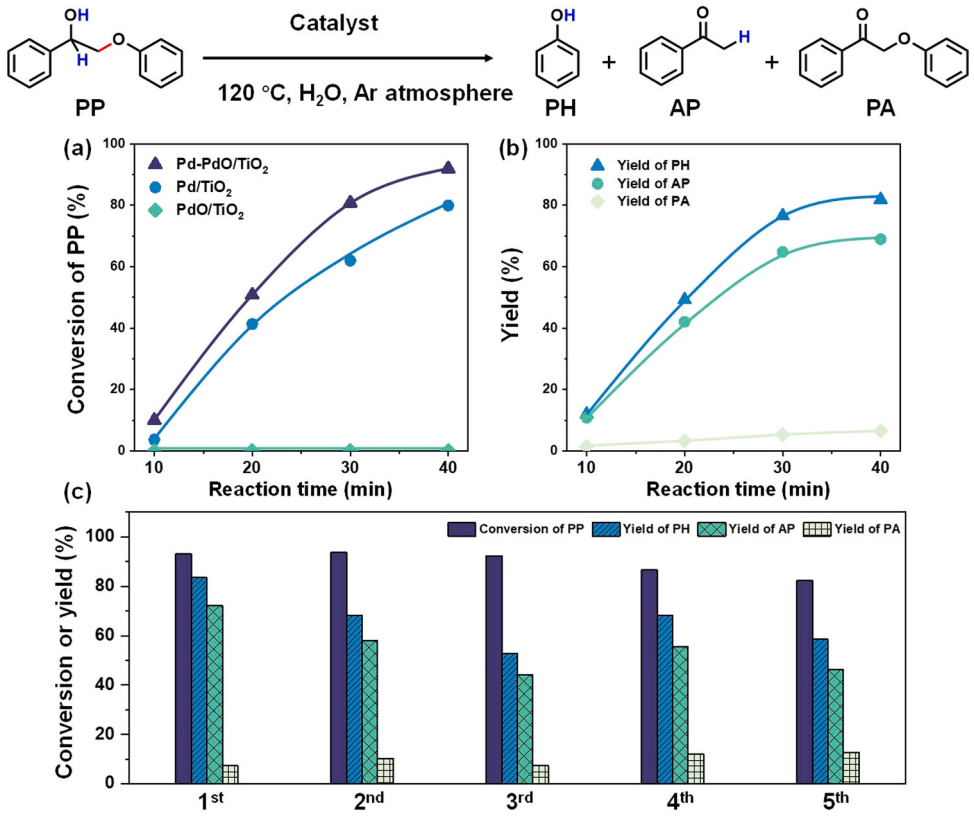

Fig. 2. (a) Reactivity of the three types of Pd/TiO_2 catalyst to STH of **PP**. (b) Time-on-course process of STH of **PP** on Pd-PdO/TiO_2 catalyst. (c) Stability test of Pd-PdO/TiO_2. Reaction conditions: 5 mg of catalyst, 20 mg of **PP**, 2 mL of H_2O, Ar atmosphere, 120 °C.

converged to −0.02 eV. The lattice constants of Pd were optimized to be 3.944 Å, in good agreement with the experimental constants 3.891. The lattice constants of PdO were optimized to be $a = b = 3.062$ Å, and $c = 5.330$ Å, in good agreement with the experimental constants, $a = b = 3.030$ Å, and $c = 5.330$ Å. We used them to build a $(6 \times 2\sqrt{3})$ Pd (111) and (3×2) Pd(110) slab with four atomic layers and a vacuum of 15 Å. Atoms in the bottom two atomic layers were fixed to their bulk positions, while the rest were allowed to fully relax.

3. Results and discussion

3.1. Characterization of catalyst

The morphology of Pd-PdO/TiO_2 was observed by HR-TEM. As shown in Fig. 1a, Pd-based nanoparticles with an average size of about 3 nm are highly dispersed on TiO_2. The detailed structure of Pd-PdO/TiO_2 can be observed in Fig. 1b. It can be seen that TiO_2 exhibits high crystallinity and clear lattice fringes. The lattice space 0.325 nm and 0.25 nm can be observed which are the spacing of the (1 0 1) plane of anatase [48] and (1 0 1) plane of rutile [49], respectively. Also, the lattice spacing of 0.235 nm for Pd (111) was observed [50]. PdO was not observed in the HR-TEM, which may be reduced by the high-energy electron beams. The Pd particle in Pd/TiO_2 and Pd-PdO/TiO_2 shows the same s similar average size distribution (2–4 nm) (Fig. S1). The crystalline phases of Pd-PdO/TiO_2 were investigated by X-ray diffraction (XRD). As shown in Fig. S2, Pd-PdO/TiO_2 gives the characteristic diffraction peaks of both anatase and rutile phases TiO_2 (PDF#37–1764, PDF#77–0440). There are no diffraction peaks assigned to Pd and PdO due to their low content and high dispersity. We then used XPS techniques to study the chemical state of PdO/TiO_2, Pd-PdO/TiO_2 and Pd/TiO_2 catalysts. As shown in Fig. 1c, the peaks at 335.1 eV and 340.5 eV were assigned to metallic Pd, while the peaks located at 337.1 eV and 342.3 eV were assigned to PdO [51]. This result indicated that Pd-PdO/TiO_2 has two different state Pd species (metallic Pd and PdO). The ratios of PdO and Pd have been calculated to be 1:3 and 1:1.2 for Pd/TiO_2 and Pd-PdO/TiO_2, respectively (Fig. S3). The hydrogen temperature-programmed reduction (H_2-TPR) experiment (Fig. 1d) showed that a reduction peak at 270 °C appeared in the curve of Pd-PdO/TiO_2 catalyst, but absent in the curve of Pd/TiO_2, further indicating that the content of PdO in Pd-PdO/TiO_2 is higher than Pd/TiO_2.

3.2. Fragmentation of lignin models

2-Phenoxy-1-phenylethanol (**PP**), a dimeric model compound of lignin, was used as a probe molecule to investigate the STH process of β-O-4 linkage in lignin. The catalytic activity of the as-prepared PdO/TiO_2, Pd-PdO/TiO_2 and Pd/TiO_2 was investigated. As shown in Fig. 2, 2-phenoxy-1-phenylethanol (**PP**) was converted into three parts, phenol (**PH**), acetophenone (**AP**), and 2-phenoxy-1-phenylethanone (**PA**). We found that Pd-PdO/TiO_2 is the most efficient catalyst for this reaction, which can convert 92% of **PP** in 40 min at 120 °C. The catalytic activity of Pd/TiO_2 was lower than that of Pd-PdO/TiO_2 and the reaction cannot proceed using PdO/TiO_2 as catalyst (Fig. 2a). These results show that the metallic Pd is essential for this reaction and PdO can improve the STH activity, indicating that the co-existence of Pd and PdO has a better catalytic performance. Then we used Pd-PdO/TiO_2 as the catalyst to measure the time-on-course process (Fig. 2b). As the reaction proceeded, **PP** was converted into **PH**, **AP** and **PA** gradually. A 92% conversion of **PP** was reached after 40 min, and the yield of phenol and acetophenone was 82% and 69% respectively, along with a 7% yield of **PA**. Furthermore, the stability of the Pd-PdO/TiO_2 catalyst was investigated (Fig. 2c). The Pd-PdO/TiO_2 catalyst was stable and could be reused five times without loss of activity. Supported Pd catalysts, especially Pd/C,

Table 1
Substrate scope of self-hydrogen transfer hydrogenolysis of C_β−O bond.

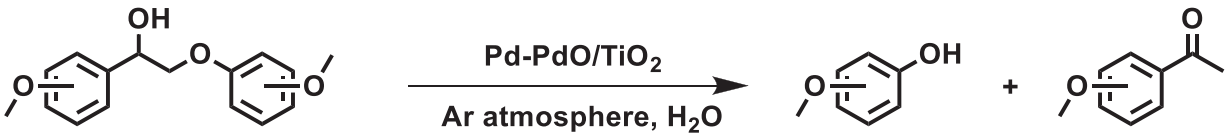

Entry	Substrate	Time (h)	T (°C)	Conv. (%)	Products and yield (%)		
1	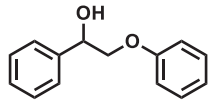	1	120	95	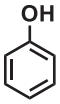 81	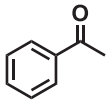 69	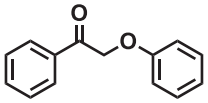 9
2	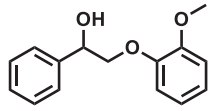	2	120	81	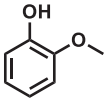 45	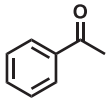 34	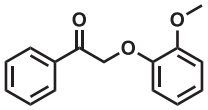 14
3	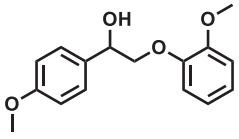	2	160	96	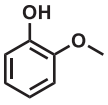 72	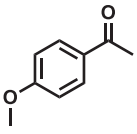 76	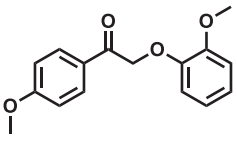 1
4	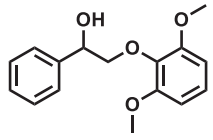	2	120	99	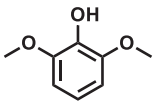 94	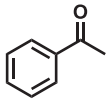 80	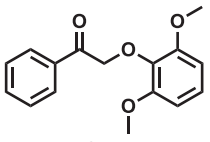 6
5	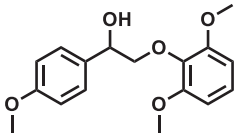	4	160	89	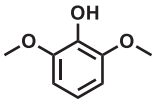 74	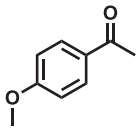 63	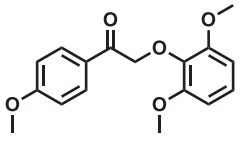 7
6	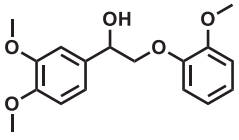	4	160	83	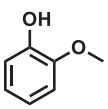 58	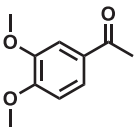 54	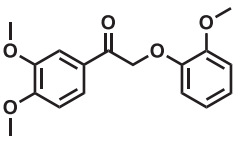 10

Reaction conditions: 20 mg of the substrate, 5 mg of Pd-PdO/TiO_2, 2 mL of H_2O, Ar atmosphere.

were widely used for the hydrogenolysis of lignin and lignin models in hydrogen atmospheres [32–38], but showed poor activity in the STH of **PP** (Fig. S4), which is probably due to the absence of stabilized PdO. The support effect was also investigated, and TiO_2 shows the best performance (Fig. S4). We then probed the generality of this STH process to other β-O-4 models with methoxy groups on the benzene ring, and 34–94% yields of the C_β-O bond cleavage products are obtained (Table 1). This result showed that the methoxy number or its position on the benzene ring affects this reaction, which may be due to the different adsorption behavior on the catalyst for different substrates.

3.3. Fragmentation of native lignin

Next, we investigate the STH of various native lignin in the aqueous phase over the Pd-PdO/TiO_2 catalyst. The lignin monomers are varied for different lignin and majorly consist of H-C0, H-C2, G-C2, G-C3, S-C3, S-C3-OH (Fig. 3). Willow and sorghum afforded 9 and 17 *wt* % lignin monomers yields. Pine is rich in G units and almost depolymerized into G-C3 and G-C2 monomers with a yield of 20 *wt* %. Poplar shows the highest lignin monomers yield with 40 *wt* %. There are about 17% p-hydroxybenzoate (PB) units in polar lignin, which can be released via hydrolysis and further converted into phenol product via

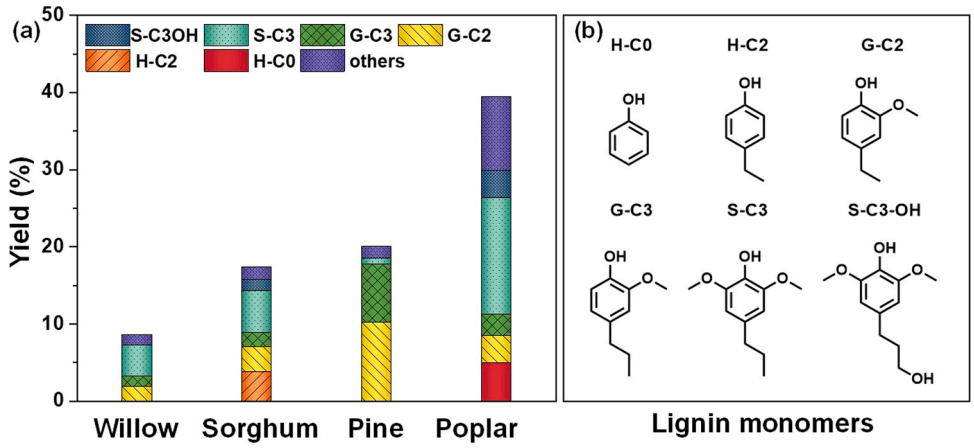

Fig. 3. Lignin monomers yield (a) and product distribution (b) from various native lignin. Reaction conditions: 0.5 g of wood powder, 50 mg of Pd-PdO/TiO_2, 10 mL of H_2O, Ar atmosphere, 180 °C, 6 h. The structure of others lignin monomers is shown in Fig. S6.

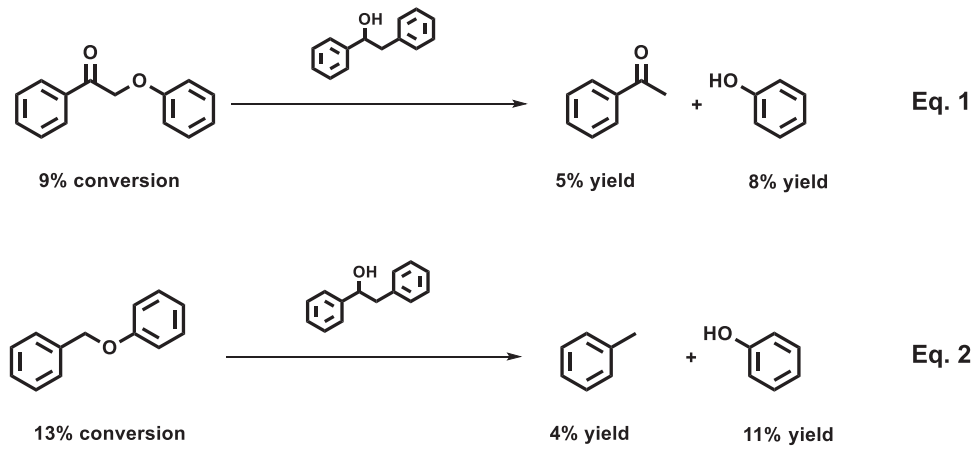

Scheme 2. Investigation of STH process. Reaction conditions: 50 mg of substrate, 50 mg of diphenylethanol, 10 mg of Pd-PdO/TiO_2, 2 mL of H_2O, Ar atmosphere, 160 °C, 6 h.

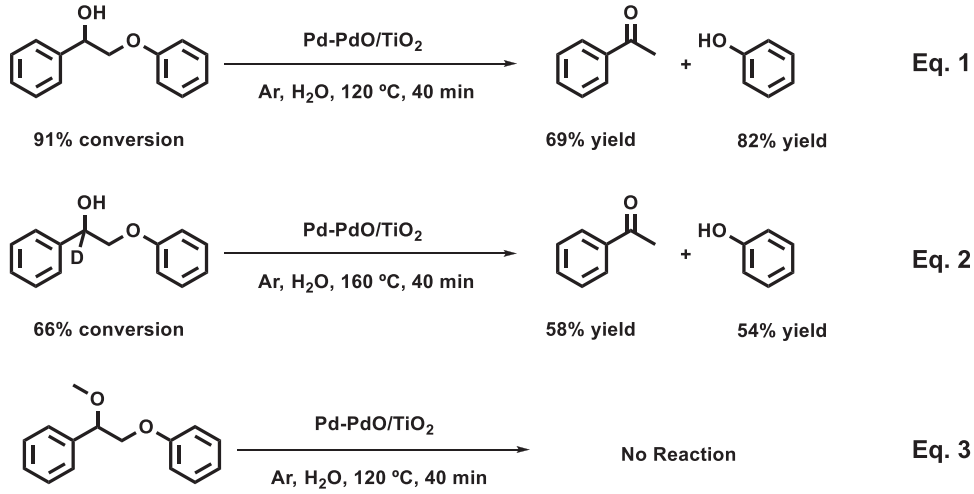

Scheme 1. Control experiments to illustrate the reaction mechanism. Reaction conditions: 20 mg of the substrate, 5 mg of catalyst, 2 mL of H_2O.

decarboxylation [7]. Other lignin linkages, such as α-O-4, can also be cleaved over the catalyst (Scheme 2, Eq. (2)). These reasons account for the high monomer yields from poplar lignin. Commercial Pd/C was previously used as a catalyst to fragment lignin samples under ambient pressure of H_2 [52]. Compared to the commercial Pd/C catalyst, the Pd-PdO/TiO_2 has a higher catalytic ability toward the STH of poplar lignin (Fig. S5, 15 *wt* % lignin monomers from poplar sawdust over Pd/C).

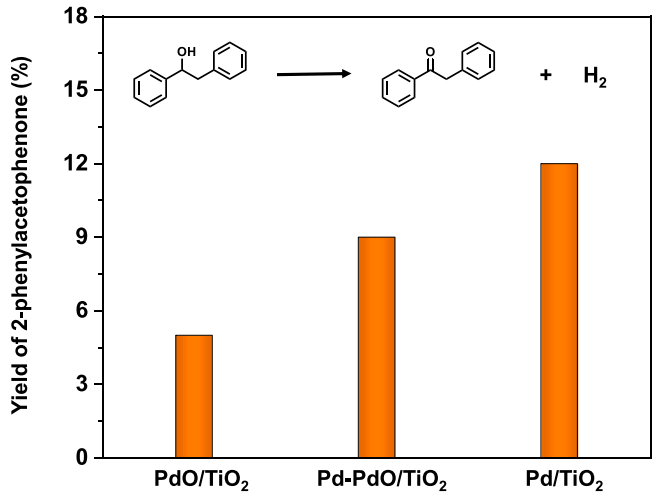

Fig. 4. Control experiment to illustrate the behavior of the catalyst during the STH process. Reaction conditions: 10 mg of diphenylethanol, 5 mg of catalyst, 2 mL of H_2O, Ar atmosphere, 120 °C, 60 min.

3.4. Reaction mechanism investigations

We conducted several mechanism verifications experiments to study the reaction mechanism. The 2-phenoxy-1-phenylethanol can be fragmented into acetophenone and phenol with yields of 69% and 82% (Scheme 1, Eq. (1)). If the substrate was replaced by deuterium substituted 2-phenoxy-1-phenylethanol on the C_α position, the fragmentation reaction became slower due to the isotopic effect. (Scheme 1, Eq. (2)). The fragmentation reaction cannot occur when the C_α-OH is replaced by C_α-OMe (Scheme 1, Eq. (3)). These results showed that the H atoms on C_αO-H and C_α-H are necessary for fragmentation of the lignin model compound, indicating an STH process of the reaction. Then, we conducted additional experiments to investigate the STH process. We used diphenylethanol (β-1 model) as the hydrogen donor, the **PA** (β-O-4 ketone model) can be fragmented to **PH** and **AP**, which indicates that the STH is not an intramolecular hydrogen transfer. The hydrogen from the hydroxyl group first forms a "hydrogen pool" on the catalyst, and then participates in the C-O bond hydrogenolysis. Moreover, we further compared the dehydrogenation step over Pd/TiO_2, $Pd\text{-}PdO/TiO_2$ and PdO/TiO_2 using diphenylethanol as the substrates (Fig. 4). Pd/TiO_2 shows the highest dehydrogenation ability which indicates that metallic Pd is the dehydrogenation site.

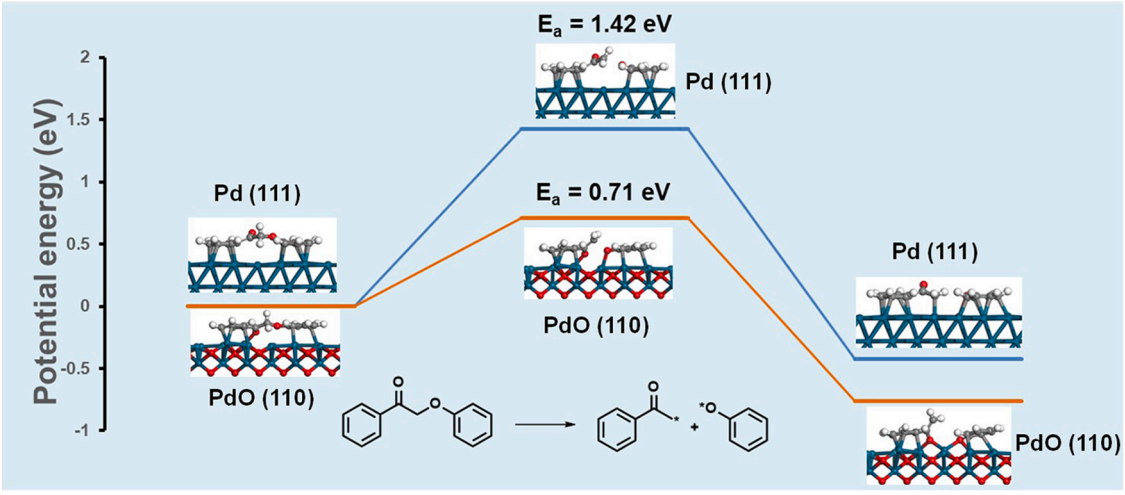

Fig. 5. DFT calculation of C-O bond cleavage of 2-phenoxy-1-phenylethanone.

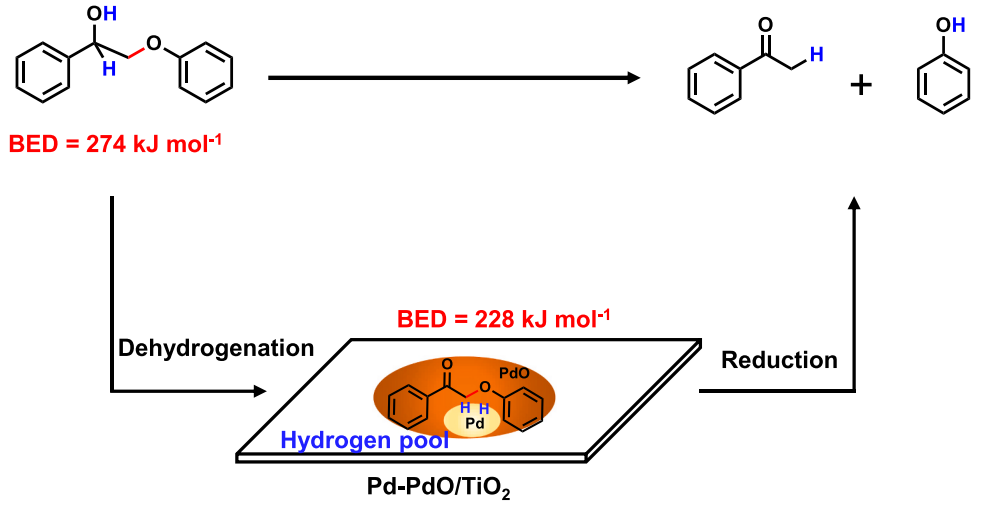

Scheme 3. Proposed mechanism for self-hydrogen transfer hydrogenation of 2-phenoxy-1-phenylethanol.

Different from the β-O-4 lignin models, most of the products from native lignin are alkylphenols and only a minor amount of ketone products was also detected (Fig. S6). Compared to β-O-4 lignin models, the native lignin provides more hydrogen. Besides the hydrogen from β-O-4 linkages, there are possible other hydrogen donors in native lignin, such as β-1 linkages. Formic acid (HCOOH) was also formed from cellulose and hemicellulose as detected by HPLC (Fig. S7). The ketone products can be further reduced to alkylphenols. With the addition of diphenylethanol (β-1 model) and formic acid, acetophenone was reduced to ethylbenzene (Fig. S8).

3.5. DFT calculations

The STH cleavage of β-O-4 is via β-O-4 ketone intermediate. We then investigated the C-O bond cleavage of 2-phenoxy-1-phenylethanone on the Pd (111) and PdO (110) surface by DFT calculation (Figs. 5 and S9 and S10). The adsorption energy (E_{ads}) of 2-phenoxy-1-phenylethanone on the Pd (111) surface is −1.64 eV. The phenyl rings adsorb on the Pd surface in a flat manner and the oxygen atoms are above the surface. A different adsorption structure was observed on PdO (110) surface and the oxygen in the C═O group binds to the surface Pd atom, making it adsorb more strongly on the surface (E_{ads} = −2.31 eV). The activation energy over PdO (110) is 0.71 eV which is lower than that over Pd (111) (1.42 eV). The DFT calculation results indicate that positively charged Pd facilitates the C_{β}−O bond cleavage of the β-O-4 ketone.

Based on the result of control experiments and the DFT calculations, we proposed a mechanism for this reaction. As shown in Scheme 3, the fragmentation reaction includes a dehydrogenation reaction and a reduction reaction. For the dehydrogenation reaction, the substrate 2-phenoxy-1-phenylethanol is dehydrogenated to 2-phenoxy-1-phenylethanone. The formation of 2-phenoxy-1-phenylethanone weakens the C_{β}−O bond via decreasing the BDE of C_{β}-O linkage from 274 kJ mol^{-1} to 228 kJ mol^{-1} [53]. At the same time, hydrogens are adsorbed on Pd sites to form a "hydrogen pool" which participates in the following reduction process. For the reduction process, the 2-phenoxy-1-phenylethanone was strongly absorbed on the PdO surface and undergoes hydrogenolysis to acetophenone and phenol by the "hydrogen pool".

4. Conclusion

In summary, we developed a Pd-PdO/TiO_2 catalyst for the hydrogen-free depolymerization of native lignin. Various β-O-4 lignin model compounds were fragmented into monomers with good yield. Lignin monomers could also be obtained from native lignin such as pine, willow, sorghum and poplar. The reaction mechanism showed that the fragmentation reaction involves two steps: dehydrogenation of C_{α}H-OH on metallic Pd to form β-O-4 ketone intermediate and a "hydrogen pool", followed by C_{β}−O bond hydrogenolysis of β-O-4 ketone intermediate by the "hydrogen pool". DFT calculation shows that PdO more effectively activates the β-O-4 ketone intermediate with lower activation energy toward C_{β}-O bond cleavage than metallic Pd. The co-existence of Pd and PdO facilitates the C_{β}−O bond cleavage of β-O-4 linkage.

CRediT authorship contribution statement

Zhaolin Dou: Conducted most of the experiments in this work, Analyzed the data. **Zhe Zhang**: Performed the catalyst characterization. **Min Wang, Zhaolin Dou**: Cowrote the manuscript. **Min Wang**: Conceived and supervised the research and revised the manuscript.

Declaration of Competing Interest

The authors declare that they have no known competing financial interests or personal relationships that could have appeared to influence the work reported in this paper.

Acknowledgments

This work was supported by the National Natural Science Foundation of China (21872135, 22002011), and China Post-doctoral Science Foundation (2020M670742).

Conflict of Interest

The authors declare no conflict of interest.

Appendix A. Supporting information

Supplementary data associated with this article can be found in the online version at doi:10.1016/j.apcatb.2021.120767.

References

[1] M. Wang, F. Wang, Catalytic scissoring of lignin into aryl monomers, Adv. Mater. 31 (2019), 1901866.
[2] R. Rinaldi, R. Jastrzebski, M.T. Clough, J. Ralph, M. Kennema, P.C.A. Bruijnincx, B. M. Weckhuysen, Paving the way for lignin valorisation: recent advances in bioengineering, biorefining and catalysis, Angew. Chem. Int. Ed. 55 (2016) 8164–8215.
[3] W. Schutyser, T. Renders, S. Van den Bosch, S.F. Koelewijn, G.T. Beckham, B. F. Sels, Chemicals from lignin: an interplay of lignocellulose fractionation, depolymerisation, and upgrading, Chem. Soc. Rev. 47 (2018) 852–908.
[4] S. Song, J. Zhang, G. Gozaydin, N. Yan, Production of terephthalic acid from corn stover lignin, Angew. Chem. Int. Ed. 58 (2019) 4934–4937.
[5] C.S. Lancefield, L.W. Teunissen, B.M. Weckhuysen, P.C.A. Bruijnincx, Iridium-catalysed primary alcohol oxidation and hydrogen shuttling for the depolymerisation of lignin, Green. Chem. 20 (2018) 3214–3221.
[6] L. Shuai, M.T. Amiri, Y.M. Questell-Santiago, F. Heroguel, Y.D. Li, H. Kim, R. Meilan, C. Chapple, J. Ralph, J.S. Luterbacher, Formaldehyde stabilization facilitates lignin monomer production during biomass depolymerization, Science 354 (2016) 329–333.
[7] M. Wang, M.J. Liu, H.J. Li, Z.T. Zhao, X.C. Zhang, F. Wang, Dealkylation of lignin to phenol via oxidation-hydrogenation strategy, ACS Catal. 8 (2018) 6837–6843.
[8] Z.H. Sun, G. Bottari, A. Afanasenko, M.C.A. Stuart, P.J. Deuss, B. Fridrich, K. Barta, Complete lignocellulose conversion with integrated catalyst recycling yielding valuable aromatics and fuels, Nat. Catal. 1 (2018) 82–92.
[9] A. Rahimi, A. Ulbrich, J.J. Coon, S.S. Stahl, Formic-acid-induced depolymerization of oxidized lignin to aromatics, Nature 515 (2014) 249–252.
[10] Y. Liao, S.-F. Koelewijn, G.Vd Bossche, J.V. Aelst, S.Vd Bosch, T. Renders, K. Navare, T. Nicolaï, K.V. Aelst, M. Maesen, H. Matsushima, J. Thevelein, K. V. Acker, B. Lagrain, D. Verboekend, B.F. Sels, A sustainable wood biorefinery for low-carbon footprint chemicals production, Science 367 (2020) 1385–1390.
[11] J. Yan, Q.L. Meng, X.J. Shen, B.F. Chen, Y. Sun, J.F. Xiang, H.Z. Liu, B.X. Han, Selective valorization of lignin to phenol by direct transformation of C-s(p2)-C-sp3 and C-O bonds, Sci. Adv. 6 (2020), eabd1951.
[12] C.Z. Li, X.C. Zhao, A.Q. Wang, G.W. Huber, T. Zhang, Catalytic transformation of lignin for the production of chemicals and fuels, Chem. Rev. 115 (2015) 11559–11624.
[13] M.M. Abu-Omar, K. Barta, G.T. Beckham, J.S. Luterbacher, J. Ralph, R. Rinaldi, Y. Román-Leshkov, J.S.M. Samec, B.F. Sels, F. Wang, Guidelines for performing lignin-first biorefining, Energy Environ. Sci. 14 (2021) 262–292.
[14] J. Zakzeski, P.C.A. Bruijnincx, A.L. Jongerius, B.M. Weckhuysen, The catalytic valorization of lignin for the production of renewable chemicals, Chem. Rev. 110 (2010) 3552–3599.
[15] M. Zaheer, R. Kempe, Catalytic hydrogenolysis of aryl ethers: a key step in lignin valorization to valuable chemicals, ACS Catal. 5 (2015) 1675–1684.
[16] S.F. Qin, B.L. Li, Z.C. Luo, C. Zhao, The conversion of a high concentration of lignin to cyclic alkanes by introducing Pt/HAP into a Ni/ASA catalyst, Green. Chem. 22 (2020) 2901–2908.
[17] C.F. Zhang, J.M. Lu, X.C. Zhang, K. MacArthur, M. Heggen, H.J. Li, F. Wang, Cleavage of the lignin beta-O-4 ether bond via a dehydroxylation-hydrogenation strategy over a NiMo sulfide catalyst, Green. Chem. 18 (2016) 6545–6555.
[18] Q. Song, J. Cai, J. Zhang, W. Yu, F. Wang, J. Xu, Hydrogenation and cleavage of the C-O bonds in the lignin model compound phenethyl phenyl ether over a nickel-based catalyst, Chin. J. Catal. 34 (2013) 651–658.
[19] X. Wang, R. Rinaldi, Exploiting H-transfer reactions with RANEY® Ni for upgrade of phenolic and aromatic biorefinery feeds under unusual, low-severity conditions, Energy Environ. Sci. 5 (2012) 8244.
[20] E.M. Anderson, M.L. Stone, M.J. Hulsey, G.T. Beckham, Y. Roman-Leshkov, Kinetic studies of lignin solvolysis and reduction by reductive catalytic fractionation decoupled in flow-through reactors, ACS Sustain. Chem. Eng. 6 (2018) 7951–7959.
[21] S. Van den Bosch, T. Renders, S. Kennis, S.F. Koelewijn, G. Van den Bossche, T. Vangeel, A. Deneyer, D. Depuydt, C.M. Courtin, J.M. Thevelein, W. Schutyser, B. F. Sels, Integrating lignin valorization and bio-ethanol production: on the role of Ni-Al_2O_3 catalyst pellets during lignin-first fractionation, Green. Chem. 19 (2017) 3313–3326.

[22] V. Molinari, G. Clavel, M. Graglia, M. Antonietti, D. Esposito, Mild continuous hydrogenolysis of kraft lignin over titanium nitride–nickel catalyst, ACS Catal. 6 (2016) 1663–1670.
[23] Q. Song, F. Wang, J. Cai, Y. Wang, J. Zhang, W. Yu, J. Xu, Lignin depolymerization (LDP) in alcohol over nickel-based catalysts via a fragmentation–hydrogenolysis process, Energy Environ. Sci. 6 (2013) 994–1007.
[24] M.R. Sturgeon, M.H. O'Brien, P.N. Ciesielski, R. Katahira, J.S. Kruger, S.C. Chmely, J. Hamlin, K. Lawrence, G.B. Hunsinger, T.D. Foust, R.M. Baldwin, M.J. Biddy, G. T. Beckham, Lignin depolymerisation by nickel supported layered-double hydroxide catalysts, Green. Chem. 16 (2014) 824–835.
[25] F.P. Bouxin, A. McVeigh, F. Tran, N.J. Westwood, M.C. Jarvis, S.D. Jackson, Catalytic depolymerisation of isolated lignins to fine chemicals using a Pt/alumina catalyst: part 1-impact of the lignin structure, Green. Chem. 17 (2015) 1235–1242.
[26] J. Zakzeski, A.L. Jongerius, P.C. Bruijnincx, B.M. Weckhuysen, Catalytic lignin valorization process for the production of aromatic chemicals and hydrogen, ChemSusChem 5 (2012) 1602–1609.
[27] W. Xu, S.J. Miller, P.K. Agrawal, C.W. Jones, Depolymerization and hydrodeoxygenation of switchgrass lignin with formic acid, ChemSusChem 5 (2012) 667–675.
[28] J. Zhang, J. Teo, X. Chen, H. Asakura, T. Tanaka, K. Teramura, N. Yan, A series of NiM (M = Ru, Rh, and Pd) bimetallic catalysts for effective lignin hydrogenolysis in water, ACS Catal. 4 (2014) 1574–1583.
[29] O.E. Ebikade, N. Samulewicz, S.Q. Xuan, J.D. Sheehan, C.Q. Wu, D.G. Vlachos, Reductive catalytic fractionation of agricultural residue and energy crop lignin and application of lignin oil in antimicrobials, Green. Chem. 22 (2020) 7435–7447.
[30] Y. Shao, Q.N. Xia, L. Dong, X.H. Liu, X. Han, S.F. Parker, Y.Q. Cheng, L.L. Daemen, A.J. Ramirez-Cuesta, S.H. Yang, Y.Q. Wang, Selective production of arenes via direct lignin upgrading over a niobium-based catalyst, Nat. Commun. 8 (2017) 16104.
[31] S. Van den Bosch, W. Schutyser, R. Vanholme, T. Driessen, S.F. Koelewijn, T. Renders, B. De Meester, W.J.J. Huijgen, W. Dehaen, C.M. Courtin, B. Lagrain, W. Boerjan, B.F. Sels, Reductive lignocellulose fractionation into soluble lignin-derived phenolic monomers and dimers and processable carbohydrate pulps, Energy Environ. Sci. 8 (2015) 1748–1763.
[32] H.L. Li, G.Y. Song, Paving the way for the lignin hydrogenolysis mechanism by deuterium-incorporated beta-O-4 mimics, ACS Catal. 10 (2020) 12229–12238.
[33] M.V. Galkin, C. Dahlstrand, J.S.M. Samec, Mild and robust redox-neutral Pd/C-catalyzed lignol-O-4 bond cleavage through a low-energy-barrier pathway, ChemSusChem 8 (2015) 2187–2192.
[34] M.V. Galkin, S. Sawadjoon, V. Rohde, M. Dawange, J.S.M. Samec, Mild heterogeneous palladium-catalyzed cleavage of β-O-4′-ether linkages of lignin model compounds and native lignin in air, ChemCatChem 6 (2014) 179–184.
[35] K. Zhang, H. Li, L.P. Xiao, B. Wang, R.C. Sun, G. Song, Sequential utilization of bamboo biomass through reductive catalytic fractionation of lignin, Bioresour. Technol. 285 (2019), 121335.
[36] X.M. Huang, O.M.M. Gonzalez, J.D. Zhu, T.I. Koranyi, M.D. Boot, E.J.M. Hensen, Reductive fractionation of woody biomass into lignin monomers and cellulose by tandem metal triflate and Pd/C catalysis, Green. Chem. 19 (2017) 175–187.
[37] K. Van Aelst, E. Van Sinay, T. Vangeel, E. Cooreman, G. Van den Bossche, T. Renders, J. Van Aelst, S. Van den Bosch, B.F. Sels, Reductive catalytic fractionation of pine wood: elucidating and quantifying the molecular structures in the lignin oil, Chem. Sci. 11 (2020) 11498–11508.
[38] T. Parsell, S. Yohe, J. Degenstein, T. Jarrell, I. Klein, E. Gencer, B. Hewetson, M. Hurt, J.I. Kim, H. Choudhari, B. Saha, R. Meilan, N. Mosier, F. Ribeiro, W. N. Delgass, C. Chapple, H.I. Kenttamaa, R. Agrawal, M.M. Abu-Omar, A synergistic biorefinery based on catalytic conversion of lignin prior to cellulose starting from lignocellulosic biomass, Green. Chem. 17 (2015) 1492–1499.
[39] J.M. Nichols, L.M. Bishop, R.G. Bergman, J.A. Ellman, Catalytic C-O bond cleavage of 2-aryloxy-1-arylethanols and its application to the depolymerization of lignin-related polymers, J. Am. Chem. Soc. 132 (2010) 12554–12555.
[40] J.W. Zhang, G.P. Lu, C. Cai, Self-hydrogen transfer hydrogenolysis of beta-O-4 linkages in lignin catalyzed by MIL-100(Fe) supported Pd-Ni BMNPs, Green. Chem. 19 (2017) 4538–4543.
[41] N.C. Luo, M. Wang, H.J. Li, J. Zhang, T.T. Hou, H.J. Chen, X.C. Zhang, J.M. Lu, F. Wang, Visible-light-driven self-hydrogen transfer hydrogenolysis of lignin models and extracts into phenolic products, ACS Catal. 7 (2017) 4571–4580.
[42] X.J. Wu, X.T. Fan, S.J. Xie, J.C. Lin, J. Cheng, Q.H. Zhang, L.Y. Chen, Y. Wang, Solar energy-driven lignin-first approach to full utilization of lignocellulosic biomass under mild conditions, Nat. Catal. 1 (2018) 772–780.
[43] L. Li, L. Dong, D. Li, Y. Guo, X. Liu, Y. Wang, Hydrogen-free production of 4-alkylphenols from lignin via self-reforming-driven depolymerization and hydrogenolysis, ACS Catal. 10 (2020) 15197–15206.
[44] G. Kresse, J. Furthmuller, Efficiency of ab-initio total energy calculations for metals and semiconductors using a plane-wave basis set, Comput. Mater. Sci. 6 (1996) 15–50.
[45] J.P. Perdew, K. Burke, M. Ernzerhof, Generalized gradient approximation made simple, Phys. Rev. Lett. 77 (1996) 3865–3868.
[46] G. Kresse, D. Joubert, From ultrasoft pseudopotentials to the projector augmented-wave method, Phys. Rev. B 59 (1999) 1758–1775.
[47] H.J. Monkhorst, J.D. Pack, Special points for brillouin-zone integrations, Phys. Rev. B 13 (1976) 5188–5192.
[48] P. Bindra, A. Hazra, Electroless deposition of Pd/Pt nanoparticles on electrochemically grown TiO_2 nanotubes for ppb level sensing of ethanol at room temperature, Analyst 146 (2021) 1880–1891.
[49] X.B. Wu, N. Qin, F. Wang, Z.H. Li, J.Y. Qin, G.J. Huang, D.H. Wang, P. Liu, Q. R. Yao, Z.G. Lu, J.Q. Deng, Reversible aluminum ion storage mechanism in Ti-deficient rutile titanium dioxide anode for aqueous aluminum-ion batteries, Energy Storage Mater. 37 (2021) 619–627.
[50] P.R. Dusane, D.S. Gavhane, P.S. Kolhe, P.K. Bankar, B.R. Thombare, G.S. Lole, B. B. Kale, M.A. More, S.I. Patil, Controlled decoration of palladium (Pd) nanoparticles on graphene nanosheets and its superior field emission behavior, Mater. Res. Bull. 140 (2021), 111335.
[51] W. Zhao, S. Liu, H.S. Wang, J. Yang, X.H. Chen, Ultrasmall Pd nanoparticles supported on TiO_2 for catalytic debenzylation via hydrogenative C-N bond cleavage, ACS Appl. Nano Mater. 4 (2021) 159–166.
[52] F. Gao, J.D. Webb, H. Sorek, D.E. Wemmer, J.F. Hartwig, Fragmentation of lignin samples with commercial Pd/C under ambient pressure of hydrogen, ACS Catal. 6 (2016) 7385–7392.
[53] M. Wang, X.C. Zhang, H.J. Li, J.M. Lu, M.J. Liu, F. Wang, Carbon modification of nickel catalyst for depolymerization of oxidized lignin to aromatics, ACS Catal. 8 (2018) 1614–1620.